REPRINTED FROM:

OPTICS COMMUNICATIONS

Optics Communications 102 (1993) 297–303
North-Holland

High-power widely-tunable picosecond pulses from an all-solid-state synchronously-pumped optical parametric oscillator

M.J. McCarthy, S.D. Butterworth and D.C. Hanna
Optoelectronics Research Centre, University of Southampton, Southampton SO9 5NH, UK

Received 10 May 1993

NORTH-HOLLAND
AMSTERDAM – LONDON – NEW YORK – TOKYO

Optics Communications 102 (1993) 297–303
North-Holland

OPTICS
COMMUNICATIONS

High-power widely-tunable picosecond pulses from an all-solid-state synchronously-pumped optical parametric oscillator

M.J. McCarthy, S.D. Butterworth and D.C. Hanna
Optoelectronics Research Centre, University of Southampton, Southampton SO9 5NH, UK

Received 10 May 1993

The operation is reported of an all-solid-state singly-resonant synchronously-pumped lithium triborate optical parametric oscillator (OPO). Two different configurations of the gain medium are reported. The first gain medium has antireflection-coated faces, and the second Brewster-angled faces. The antireflection-coated (Brewster-angled) device had an oscillation-threshold average pump power of 90 mW (170 mW) at 523 nm. At 2.8 (1.9) times threshold, the pump depletion was 50% (60%), and the oscillator converted 30% (34%) of the pump radiation into tunable output in pulses of ~1 ps duration. Temperature-tuned noncritical phase matching in the parametric oscillator yielded radiation continuously tunable over the range 0.85–1.36 μm (0.72–1.91 μm) with up to 43 mW (89 mW) of average power in the resonated wave output, and 33 mW (44 mW) in the nonresonated wave output.

1. Introduction

The synchronously-pumped optical parametric oscillator (OPO) is potentially the ideal source for the many applications requiring widely-tunable ultrashort pulses, e.g. ultrafast spectroscopy. For high signal-to-noise ratio in ultrafast spectroscopy, a high pulse repetition rate is advantageous. Consequently, a continuous-wave (cw) pump source is desirable. From the point of view of amplitude and frequency stability in the OPO output, it is desirable to resonate only one of the generated waves in a singly-resonant oscillator (SRO).

Singly-resonant synchronously-pumped OPO's have been demonstrated using a variety of main frame lasers as the pump source [1–7]. To date, the most efficient performance has been obtained from OPO's utilising potassium titanyl phosphate (KTP) as the gain medium and synchronously pumped by titanium sapphire lasers [5–7]. Using an angle-tuned critically-phase-matched parametric interaction, Fu et al. and Pelouch et al. have achieved pulses of ~100 fs duration tunable over the range 1.2–1.4 μm and 1.8–2.2 μm [5,6]. Nebel et al. achieved pulses of ~1 ps or ~400 fs duration tunable over the range 1.05–1.22 μm and 2.29–2.87 μm using a noncritically-phase-matched interaction and tuning of the pump laser wavelength [7]. All these devices supplied average output powers of several hundred milliwatts in both the signal and idler branches.

For a compact and efficient device, a laser diode pump source is desirable. Singly-resonant synchronously-pumped OPO's have been reported with cw mode-locked all-solid-state pump sources based on laser-diode-pumped Nd:YLF lasers. A system based on quasi-noncritically phase matched KTP was reported by us [8]. Angle tuning of the oscillator achieved output tunable over the range 1.0–1.1 μm with pulses of ~1 ps duration and output powers of 30–40 mW.

Lithium triborate (LBO) has the attractive properties of widely-temperature-tunable noncritical phase matching and very low material dispersion across the visible and near infrared regions of the electromagnetic spectrum. With temperature-tuned noncritical phase matching, wide tuning can be achieved without the introduction of large Poynting vector walk-off. This allows the use of tightly focused beams across the entire tuning range. Low chromatic dispersion means that the material has a large spectral-acceptance bandwidth–length product and low group-velocity walk-off between the interacting pulse

profiles. Thus a long crystal length can be effectively used. These properties make LBO particularly suitable as the gain medium for a widely-tunable SRO synchronously pumped by a mode-locked laser-diode-pumped source which would typically deliver low peak power picosecond pulses. Robertson et al. demonstrated an OPO with a laser-diode-pumped source using LBO as the gain medium [9]. They reported the impressive tuning range of 0.65–2.7 μm, with an oscillation-threshold average pump power of 150 mW and output powers of ~1 mW. We recently reported the efficient and widely-tunable operation of an LBO SRO, delivering pulses of ~1 ps duration tunable over the range 0.81–1.48 μm. The oscillation-threshold pump power was 70 mW, with average output powers of up to 80 mW being achieved [10]. However, in that work we only coupled out the longer wavelength nonresonated wave as an output for the OPO. In addition, the OPO performance dropped when tuned away from degeneracy due to the increasing reflection loss from the antireflection (AR) coatings on the LBO crystal at the resonant wavelength.

Here, we report the operation of a singly-resonant synchronously-pumped LBO OPO in which both of the generated waves could be simultaneously and efficiently accessed as outputs. The OPO has been operated in two configurations; the first utilised a standard AR-coated LBO crystal; the second used a Brewster-angled LBO crystal as the gain medium. The latter configuration avoided the well known problems associated with AR coatings on LBO (both adhesion and spectral roll-off), and allowed essentially constant output across a broad tuning range. With the frequency-doubled output of a passively-mode-locked laser-diode-pumped Nd:YLF laser as the pump source, pulses of ~1 ps duration were obtained from the OPO. The Brewster-angled OPO was tunable over the range 0.72–1.91 μm, with average output powers as high as 89 mW and pump depletions of 60%.

2. Experimental arrangement

The laser pump source was a frequency-doubled self-starting additive-pulse-mode-locked Nd:YLF laser pumped by a laser diode, as described in detail previously [8]. Minor alterations to the configuration described in ref. [8] included lengthening the laser cavity from 1.2 m to 1.4 m, and reducing the fibre length in the external cavity to 0.65 m. With a 3 W laser diode at the pump wavelength of 798 nm, the Nd:YLF laser produced in excess of 500 mW of average output power in transform-limited pulses of 2.0 ps duration at the laser wavelength of 1047 nm. This corresponds to a pulse peak power of 2.2 kW. Efficient frequency doubling was achieved using a 12 mm long LBO crystal in an external resonant enhancement cavity. The LBO crystal was AR coated on both entrance and exit faces at both 1047 nm and 523 nm. The LBO crystal was mounted in an oven for temperature-tuned noncritical phase matching. With 440 mW of average power at 1047 nm incident onto the enhancement cavity, 350 mW of average power at 523 nm could be routinely obtained corresponding to an external conversion efficiency of ~80%. The second harmonic output was in pulses of 2 ps duration, representing a pulse peak power of 1.6 kW.

The OPO cavity was a linear configuration as shown in fig. 1. The two curved mirrors and one of the plane mirrors were coated to be highly reflecting ($R > 99.9\%$) at the resonated wavelength, and highly transmitting at the pump wavelength of 523 nm ($T > 96\%$). The plane high reflector was mounted on a piezo-electric transducer for fine cavity length control. The fourth mirror was a planar output coupler with a transmission of ~3% at the resonated wavelength. This mirror was mounted on a micrometer-driven translation stage for coarse control of the OPO

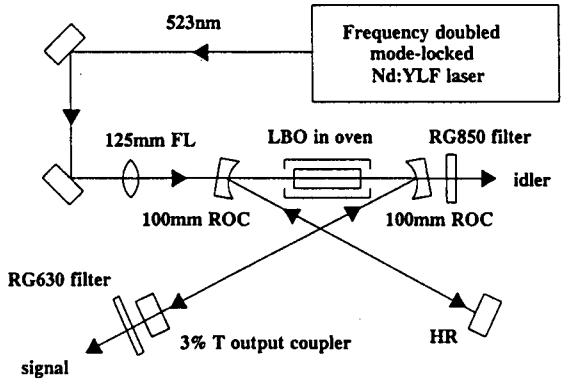

Fig. 1. Schematic diagram of the OPO.

cavity length. Two mirror sets were available, covering the spectral ranges 700–850 nm and 800–1000 nm. Both of the LBO crystals used in the OPO were cut for temperature-tuned noncritical phase-matching propagating along the crystallographic x axis. The LBO crystals were mounted in ovens which could vary the crystal temperature between ambient and ~200°C with a stability of ±0.1°C. Care was taken to ensure minimal thermal gradients within the crystals at elevated temperatures. The temperature-acceptance width for the 12 mm long AR/AR LBO crystal for second harmonic generation was measured to be 2.9°C, as shown in fig. 2, and 2.7°C for the 13 mm long Brewster crystal. The calculated temperature acceptance widths using the temperature-dependent dispersion relations of Lin et al. [11] were calculated to be 2.8°C and 2.6°C, respectively, indicating that the experimental results confirm an absence of significant temperature gradients within the crystals.

3. Antireflection-coated LBO OPO

The AR/AR LBO crystal was 3×3 mm² aperture×12 mm long. The crystal was AR coated on both entrance and exit faces at 1047 nm and 523 nm. The reflectivity at 1047 nm was 0.4% per surface, and 3.1% per surface at 523 nm. Thus, the round-trip loss for the resonated wave was ~5.6% (output coupler transmission ~4%) close to degeneracy. The angle of incidence on the curved mirrors was kept to 2.5° to minimise astigmatism in the cavity. The LBO crystal was placed at the intracavity focus between the two curved mirrors where the resonated mode waist was designed to be 26 μm radius ($1/e^2$ intensity). With a 125 mm focal length lens, the incident 523 nm pump beam was focused down to a 16 μm waist within the LBO crystal. At a resonated wavelength of 970 nm, the reflection loss of the LBO crystal was 0.5% per surface, giving a round trip reflection loss of 5.0% for the resonated wave. The oscillation threshold pump power at 523 nm for this resonated wavelength was 90 mW incident on the pump focusing lens as shown in fig. 3. This corresponds to a pulse peak power of 410 W, and a power density of 100 MW cm^{-2}. The slope efficiency for the resonated wave with respect to the pump power incident on the pump focusing lens was 36%, with an average output power of 43 mW for the resonated

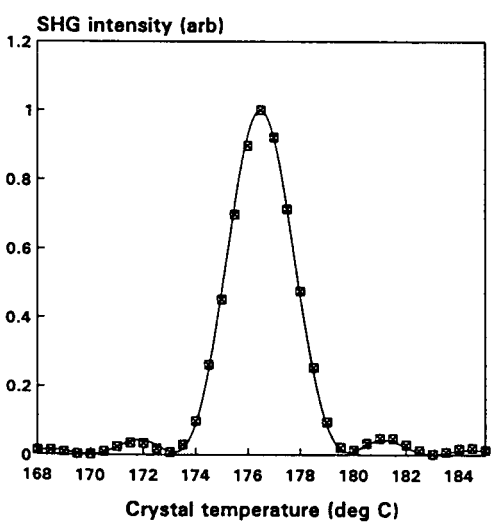

Fig. 2. Variation of the second harmonic generation (SHG) intensity with temperature for the 12 mm long AR coated LBO crystal. The temperature acceptance width (fwhm) of the sinc² fit to the data points is 2.9°C; –: sinc² fit, ⊠: data points.

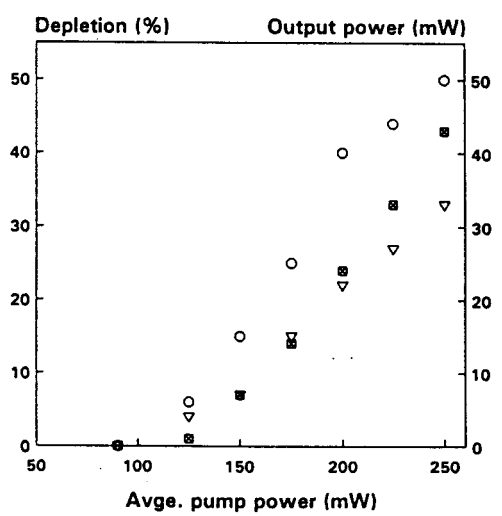

Fig. 3. Variation of the resonated and nonresonated wave average output power, and the pump depletion, with average pump power for the AR LBO OPO; ⊠: resonated wave, ○: pump depletion, ▽: nonresonated wave.

wave at 970 nm through the output coupler for 250 mW pump power corresponding to operation at 2.8 times above threshold. In addition, 33 mW of the nonresonated wave at 1140 nm was coupled out through the rear curved mirror. This corresponds to a total external conversion efficiency of 30%. At this pumping level, the pump depletion was 50%.

Measurements of the OPO output pulse duration were made by intensity autocorrelation through second harmonic generation in a 2 mm thick $LiIO_3$ crystal originally cut for frequency doubling 1.3 μm radiation to 0.65 μm. Autocorrelation measurements of the output pulse train fitted accurately to a $sech^2$ profile. At the resonated wavelength of 970 nm, the resonated wave autocorrelation width was 1.9 ps, corresponding to a pulse duration of 1.2 ps. The OPO bandwidth was 1.5 nm giving a time–bandwidth product of 0.9, indicating excess bandwidth. This was confirmed by interferometric autocorrelations, where the loss of coherence in the steeply rising wings of the autocorrelation was indicative of nontransform-limited pulses.

The OPO was tuned by varying the temperature of the crystal oven over the range 175–150°C. In tuning the OPO, small length adjustments were the only alterations necessary to the OPO cavity to account for optical path length changes in the crystal. Realignment of the OPO cavity, as required with angle tuning, was not necessary. The tuning behaviour of the OPO was monitored with a grating optical spectrum analyzer having a resolution of 0.1 nm. The OPO mirrors only allowed the shorter wavelength wave to be resonated thus ensuring singly resonant operation over the tuning range. Under this singly resonant operation, the OPO spectrum showed a single peak, and was of a smooth profile over the tuning range. In addition, the singly resonant operation resulted in excellent amplitude stability in the OPO output. Using only the long wavelength mirror set, the tuning range for the resonated wave in the AR coated LBO OPO was 850–980 nm, with the nonresonated wave tuning over the range 1120–1360 nm. The OPO output dropped on tuning away from degeneracy, primarily due to the antireflection coatings on the LBO crystal becoming increasingly ineffective at the resonated wavelength, e.g. at 850 nm, the round trip reflection loss from the LBO crystal had increased to 6.8%.

4. Brewster-angled LBO OPO

Since the efficiency and tuning range of the OPO was limited by the AR coatings on the LBO crystal, we replaced the AR coated crystal with a Brewster angled crystal, for which the reflection loss for the resonated wave would be considerably reduced across the entire tuning range. The Brewster angled crystal was 3×3 mm^2 aperture×13 mm long. The crystal

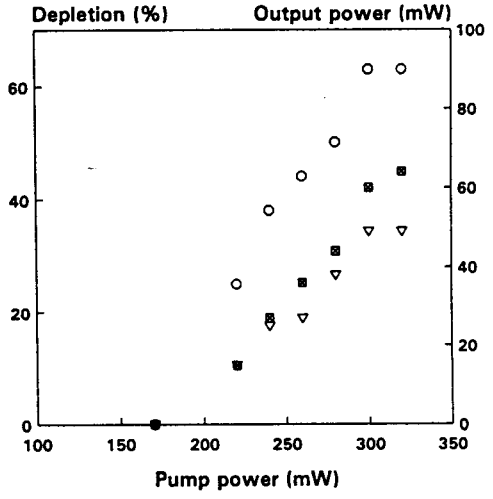

Fig. 4. Variation of the resonated and nonresonated wave average output power, and the pump depletion, with average pump power for the Brewster-angle LBO OPO; notation as in fig. 3.

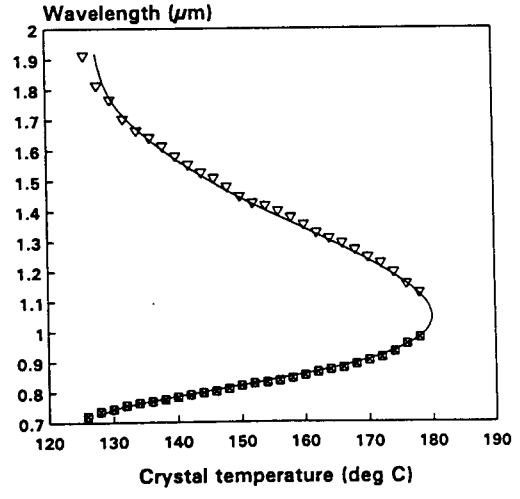

Fig. 5. Temperature tuning behaviour of the Brewster-angle LBO OPO. The solid line is the calculated behaviour based on the temperature-dependent dispersion relations of Lin et al. The symbols are data points; ⊠: resonated wave, ▽: nonresonated wave, –: calculated.

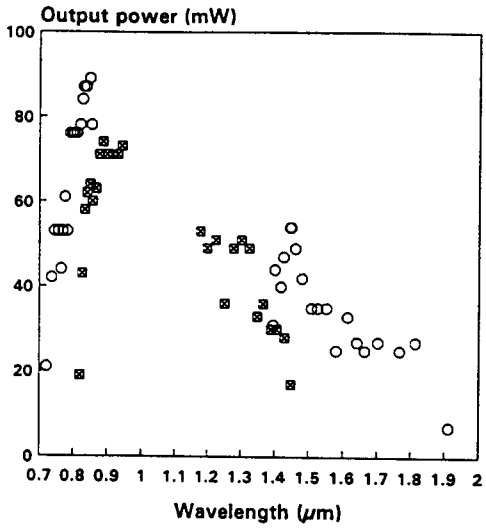

Fig. 6. Variation of the Brewster-angle LBO OPO average output power for both the resonated and the nonresonated waves across the tuning range; O: 750–850 nm set, ⊠: 800–100 nm set.

was of rather poor quality, with a total single pass loss of 0.8%, the reflection loss from each Brewster surface contributing only 0.1% loss. Careful transverse positioning of the Brewster crystal was required to locate a beam path giving acceptable performance. The angle of incidence on the curved mirrors was increased to 13° to compensate for the astigmatism introduced into the OPO cavity by the LBO crystal [12]. The calculated waist size for the resonated beam in the LBO crystal was 26 μm×41 μm, with the circular waist on the 3% transmission output coupler remaining at 450 μm. Using the two different mirror sets, the oscillation-threshold average pump power was measured at three different resonated wavelengths (960 nm, 870 nm, 855 nm) to be 170 mW average power. The slope efficiency for the resonated wave was ~40%, corresponding to an average output power of 64 mW for the resonated wave at 870 nm for an average pump power of 320 mW, as shown in fig. 4. In addition, 50 mW of average power for the nonresonated wave at 1320 nm was coupled out through the rear curved mirror. At this pump level, the pump depletion was 63%.

Using the two mirror sets, the resonated wave was temperature tuned over the ranges 978–816 nm and 853–721 nm. The nonresonated wave tuned over the corresponding ranges 1126–1460 nm and 1355–1191 nm. The entire temperature tuning range is shown in fig. 5. The average output power for the OPO across the tuning range is shown in fig. 6. The resonated

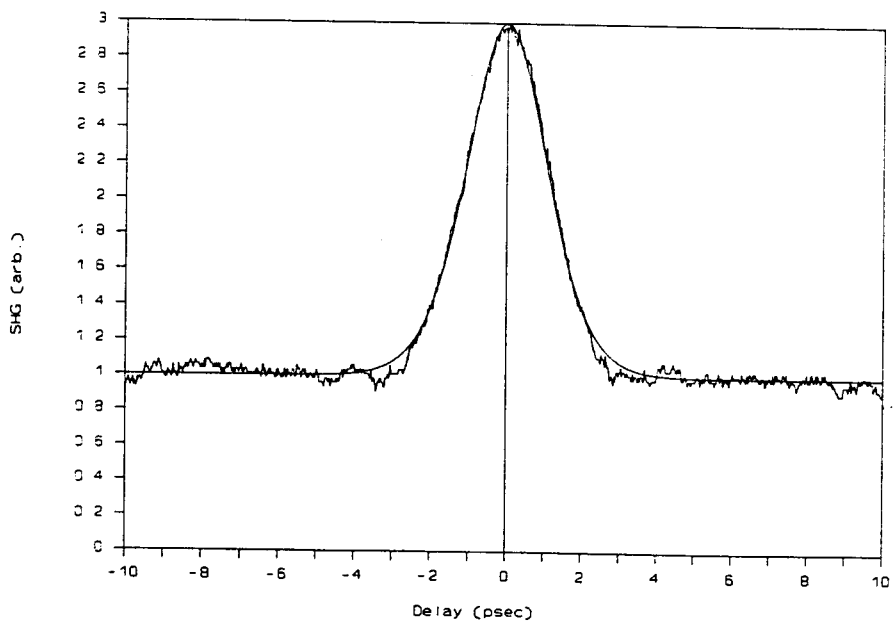

Fig. 7. Autocorrelation profile of the resonated wave output pulse train for the Brewster-angle LBO OPO. The smooth curve is a sech^2 fit to the data, with a fwhm of 2.5 ps. This corresponds to a pulse duration of 1.6 ps; –: sech^2 fit.

wave output power through the output coupler was > 50 mW over the range 978–744 nm, with the non-resonated wave output power through the rear curved mirror being > 30 mW over the range 1164–1813 nm. Again, the singly-resonant nature of the oscillator resulted in both excellent amplitude stability and the OPO spectrum exhibiting a single peak.

Autocorrelation measurements of the output pulse train again fitted accurately to a sech^2 profile. At the resonated wavelength of 785 nm, the resonated wave autocorrelation width was 2.5 ps, as shown in fig. 7. The deconvoluted pulse duration was 1.6 ps. The corresponding spectrum, shown in fig. 8, had a fwhm of 1.2 nm. The time–bandwidth product was again ~0.9 indicating that the pulses had a time–bandwidth product approximately three times the transform limited value.

The variation of the LBO OPO output power with OPO cavity length detuning was observed to follow that of the KTP OPO [1]. Thus the output power dropped rapidly when tuning to longer OPO cavity lengths from optimum length detuning, and dropped more slowly when detuning to shorter cavity lengths. The OPO could withstand a total cavity length detuning of 28 μm before oscillation ceased. In contrast to the KTP OPO, the output pulse train showed little variation in duration or chirp with cavity length detuning. In addition, the oscillating wavelength of the LBO OPO could be tuned over a range of ~50 nm by length-tuning the OPO cavity over its entire range, again in contrast to the KTP OPO.

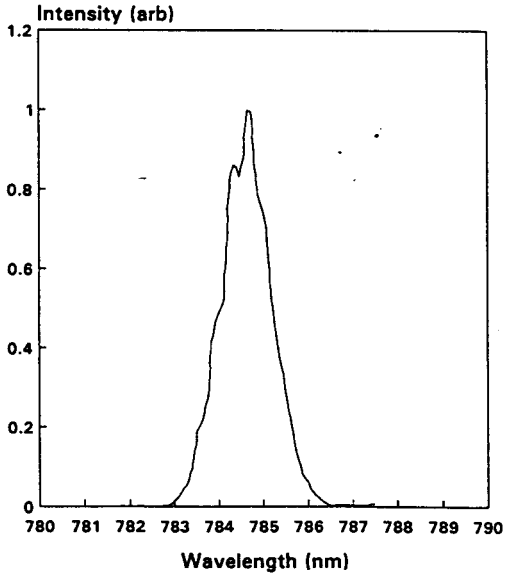

Fig. 8. Spectral output of the Brewster-angle LBO OPO corresponding to the autocorrelation data of fig. 7. The spectral fwhm is 1.2 nm.

5. Conclusion

We have demonstrated efficient, widely-tunable operation of a synchronously-pumped OPO in LBO with an all-solid-state laser pump source. Both oscillators demonstrated many of the predicted properties for LBO and in particular, confirmed its suitability for laser diode pumping. The Brewster-angled OPO in particular has shown very efficient operation across a large portion of its potential tuning range in spite of the poor quality of the crystal used in these experiments. The tuning range so far demonstrated (0.72–1.91 μm) is limited by the available mirror sets, and could therefore be extended to cover the range 0.65–2.7 μm.

We are at present looking into methods of controlling the excess bandwidth of the OPO so as to generate transform-limited pulses. One possible avenue of progression is to drive the OPO with shorter pump pulses to use the remaining spectral-acceptance bandwidth of the LBO crystal. This would also have the additional advantage of reducing the oscillation-threshold average pump power by a factor of ~3. Alternatively, the spectral-acceptance bandwidth of the OPO could be reduced by using a longer LBO crystal. Again, this would have the beneficial effect of a reduction in the oscillation-threshold average pump power, again by a factor of ~3 in principle if a three times longer crystal were used. Retaining the present arrangement, it should be possible to effect bandwidth control through the introduction of a prism sequence [13]. If the behaviour of our OPO were to follow that of femtosecond OPOs demonstrated by others [5,6], where the introduction of a prism sequence resulted in approximately transform-limited output pulses significantly shorter than the pump pulses, transform-limited pulse formation of ~500 fs duration could result. However, this would increase the complexity of the arrangement and would have little effect on the threshold power

requirements. In addition, we are looking into methods of active stabilisation of the OPO cavity length, to stabilise the oscillating wavelength and to improve the long term stability of the OPO. Thus with a few modifications to the OPO, this device should become a practical and reliable source of subpicosecond pulses across the entire tuning range of 0.65–2.7 μm.

Acknowledgements

This research has been supported by the UK Science and Engineering Research Council, which S.D. Butterworth thanks for support in the form of a CASE research studentship with Lumonics Ltd.

References

[1] D.C. Edelstein, E.S. Wachman and C.L. Tang, Appl. Phys. Lett. 54 (1989) 1728.
[2] E.S. Wachman, D.C. Edelstein and C.L. Tang, Optics Lett. 15 (1990) 136.
[3] E.S. Wachman, W.S. Pelouch and C.L. Tang, J. Appl. Phys. 70 (1991) 1893.
[4] G. Mak, Q. Fu and H.M. van Driel, Appl. Phys. Lett. 60 (1992) 542.
[5] Q. Fu, G. Mak and H.M. van Driel, Optics Lett. 17 (1992) 1006.
[6] W.S. Pelouch, P.E. Powers and C.L. Tang, Optics Lett. 17 (1992) 1070.
[7] A. Nebel, C. Fallnich and R. Beigang, Topical meeting on Advanced Solid State Lasers, New Orleans LA, 1993, paper MA4.
[8] M.J. McCarthy and D.C. Hanna, Optics Lett. 17 (1992) 402.
[9] A. Robertson, G.P.A. Malcolm, M. Ebrahimzadeh and A.I. Ferguson, Conference on Lasers and Electro-optics, Anaheim CA, 1992, paper CPD15.
[10] S.D. Butterworth, M.J. McCarthy and D.C. Hanna, Topical Meeting on Advanced Solid State Lasers, New Orleans LA, 1993, paper PD10.
[11] S. Lin, J.Y. Huang, J. Ling, C. Chen and Y.R. Shen, Appl. Phys. Lett. 59 (1991) 2805.
[12] H.W. Kogelnik, E.P. Ippen, A. Dienes and C.V. Shank, IEEE J. Quantum Electron. QE-8 (1972) 373.
[13] R.L. Fork, O.E. Martinez and J.P. Gordon, Optics Lett. 9 (1984) 150.